International Journal of Biological Macromolecules 248 (2023) 125921

Contents lists available at ScienceDirect

International Journal of Biological Macromolecules

journal homepage: www.elsevier.com/locate/ijbiomac

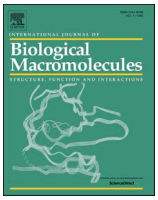

Insight into gene expression associated with DNA methylation and small RNA in the rhizome-root system of Moso bamboo

Feihu Xi [a,1], Zeyu Zhang [b,1], Lin Wu [a], Baijie Wang [a], Pengfei Gao [b], Kai Chen [a], Liangzhen Zhao [a], Jian Gao [c,*], Lianfeng Gu [b,*], Hangxiao Zhang [b,*]

[a] College of Life Science, Basic Forestry and Proteomics Research Center, Fujian Agriculture and Forestry University, Fuzhou 350002, China
[b] College of Forestry, Basic Forestry and Proteomics Research Center, School of Future Technology, Fujian Agriculture and Forestry University, Fuzhou 350002, China
[c] International Center for Bamboo and Rattan, Key Laboratory of Bamboo and Rattan Science and Technology, State Forestry Administration, Beijing, China

ARTICLE INFO

Keywords:
Moso bamboo
Rhizome-root system
Rapid growth

ABSTRACT

Moso bamboo (*Phyllostachys edulis*), typically a monopodial scattering bamboo, is famous for its rapid growth. The rhizome-root system of Moso bamboo plays a crucial role in its clonal growth and spatial distribution. However, few studies have focused on rhizome-root systems. Here we collected LBs, RTs, and RGFNSs, the most important parts of the rhizome-root system, to study the molecular basis of the rapid growth of Moso bamboo due to epigenetic changes, such as DNA modifications and small RNAs. The angle of the shoot apical meristem of LB gradually decreased with increasing distance from the mother plant, and the methylation levels of LB were much higher than those of RT and RGFNS. 24 nt small RNAs and mCHH exhibited similar distribution patterns in transposable elements, suggesting a potential association between these components. The miRNA abundance of LB gradually increased with increasing distance from the mother plant, and a negative correlation was observed between gene expression levels and mCG and mCHG levels in the gene body. This study paves the way for further exploring the effects of epigenetic factors on the physiology of Moso bamboo.

1. Introduction

Moso bamboo (*Phyllostachys edulis*) is an important fast-growing non-timber forest product worldwide. The early development and proliferation of this plant depend on an intricate underground rhizome-root system, which runs radially from the mother plant [1]. Bamboo establishes this network of underground rhizomes to absorb, store, and transport water and nutrients. The plants are also connected by their above- and below-ground parts, including shoots, culms, rhizomes, and buds. Benefiting from this powerful rhizome-root system, spring shoots can reach 20 m in height within 45–60 days, with a peak growth rate of ~1 m per day [2]. Bamboo rhizomes are typically classified into three major types based on their growth patterns: amphipodial, monopodial, and sympodial [3,4]. Moso bamboo is a scattered bamboo with monopodial rhizomes that grow horizontally at a staggering rate.

The underground rhizome-root system in bamboo generates the shoot system, which holds significant value. Multiple studies have recently been conducted to investigate the cell biology and molecular regulatory mechanism of the growth and development of bamboo shoots. For example, internode 18 of Moso bamboo shoots has been recognized as a representative internode for rapid growth [5]. Morphological studies of bamboo internodes have revealed three distinct zones: the division zone, elongation zone, and elongation completion zone [1]. Notably, different phytohormones are present at different levels in the cell division and cell elongation zones [6]. Defects in brassinosteroid (BR) signaling were associated with dwarf internodes in a slow-growing bamboo variant [7]. Furthermore, the accumulation of abscisic acid (ABA) and salicylic acid has been observed in the senescing sheath, which is associated with internode growth [8]. Gibberellic acid (GA) is a key factor determining internode elongation in monocots [9]. We previously demonstrated that the exogenous application of GA_3 elongated internodes in Moso bamboo seedlings [10]. GA_4 treatment increased cell number and cell length in Moso bamboo, and ABA and mechanical pressure may stimulate the rapid thickening of the secondary cell wall via the transcription factor MYB83L [5]. High-throughput small RNA sequencing and degradome sequencing of both wild-type Moso bamboo and a thick-walled variant revealed that miRNA–transcription factor–phytohormones regulatory networks are key players in tissue differentiation in bamboo shoots [11].

* Corresponding authors.
E-mail addresses: gaojianicbr@163.com (J. Gao), lfgu@fafu.edu.cn (L. Gu), zhanghx@fafu.edu.cn (H. Zhang).
[1] These authors contributed equally to this work.

https://doi.org/10.1016/j.ijbiomac.2023.125921
Received 11 May 2023; Received in revised form 7 July 2023; Accepted 19 July 2023
Available online 25 July 2023

Abbreviations

LB	Lateral bud
RT	Rhizome tip
RGFNS	Roots growing from new shoots
SAM	Shoot apical meristem
DMRs	Differentially methylated regions
FC	Fold change
RPM	Reads per million mapped reads
DEGs	Differentially expressed genes
GO	Gene Ontology
WGBS	Whole-genome bisulfite sequencing
TSS	Transcription start site
TTS	Transcription termination site
TEs	Transposable elements

The growth and development of the underground system of Moso bamboo is regulated by phytohormones [4] and a variety of factors [12]. Environmental factors, such as nitrogen content [13], moisture conditions [14], and light exposure [15], regulate lateral bud development. Among phytohormones, high concentrations of GAs, zeatin, and indole acetic acid (IAA) are major players in the rhizome bud. A high concentration of IAA is associated with rhizome bud outgrowth, and the formation of the bamboo shoot from the rhizome bud is driven by a high concentration of zeatin [4]. Transcriptome analysis showed that multiple pathways, such as meristem development, sugar metabolism, and phytohormone signaling pathways, are involved in the development of rhizome lateral buds [16]. Despite the importance of understanding the molecular mechanism of the rhizome-root system, little systematic research, especially epigenetic research, has been performed in this system. Epigenetic modifications, such as DNA methylation and non-coding RNA regulation, can affect the expression of genes with significant impacts on developmental processes [17,18]. DNA methylation contributes to the development of Moso bamboo from the vegetative to floral growth stage [19]. Small RNAs directly modulate gene expression in plants primarily via the siRNA-directed DNA methylation pathway [20,21]. However, little is known about the roles of DNA methylation and small RNAs in regulating the development of the underground rhizome-root system. Therefore, there is a need to investigate how methylation affects the physiology of the underground rhizome-root system in bamboo.

Here, we collected three typical parts of the rhizome-root system of Moso bamboo for morphological observation, including lateral buds (LB), rhizome tips (RT), and roots growing from new shoot (RGFNS). We further divided LB into three distinct types including proximal LB, middle LB, distal LB. The angle of the shoot apical meristem (SAM) of LB decreased with increasing distance from the mother plant. The levels of mCG, mCHG, and mCHH methylation of the protein-encoding genes and transposons were much higher in LB than in RT and RGFNS based on high-throughput whole-genome bisulfite sequencing. We also analyzed small RNAs, finding a similar distribution pattern of small RNAs and mCHH in transposable elements (TEs). MiRNA abundance in LB was positively correlated with the distance from the mother plant. We also observed a negative correlation between gene expression levels and the levels of mCG and mCHG methylation in the gene body. Studying the molecular mechanism and regulatory network of DNA methylation and small RNAs underlying the development of Moso bamboo provides a theoretical basis for the efficient cultivation of bamboo shoots and timber forests.

2. Materials and methods

2.1. Plant materials

Fresh rhizome-root tissues of Moso bamboo, including RGFNS, RT, and LB, were collected from Nanping City (26°29′–27°02′N, 118°01′–119°34′E) in Fujian province, China in 2019. Fresh tissues were snap frozen with liquid nitrogen and stored at −80 °C for analysis.

2.2. Morphology analysis

The morphology of Moso bamboo tissues was observed with a Canon EOS 70D (Canon, Tokyo, Japan) digital device and by scanning electron microscopy (Hitachi, TM3030). The angles of the SAMs in LB were determined using Angle Tool in ImageJ (1.53c) [22]. The correlation of SAM angle with LB position was analyzed and visualized with R (https://www.r-project.org).

2.3. Preparing paraffin sections and light microscopy

Fresh tissue samples were fixed in FAA buffer (10 % formalin: 50 % ethanol = 1: 5, *v*/v) and placed in a vacuum chamber (ThermoFisher, 5300–0507) for 15 min. The samples were embedded in paraffin (Leica, Cat no. 39601095) using a Leica embedding station (Leica, EG1150H). Paraffin-embedded issues were cut into 8 μm-thick section, plated on adhesion microscope slides (CITOTEST, #Cat no. 188105), and stained with safranin (Solarbio, #Cat no. S8020) and fast green (Solarbio, #Cat no. F8130). Images were taken with a Leica DFC 550 camera under a stereomicroscope (Leica, M205FA).

2.4. Extraction and quality control of genomic DNA and total RNA

Samples were homogenized in a grinding jar set (QIAGEN, #Cat no. 69985) on a High-throughput TissueLyser (QIAGEN, #Cat no. 85300) at a frequency of 30 times/s for 2 min. Genomic DNA (gDNA) was prepared using a Plant Genomic DNA Extraction kit (TIANGEN, #Cat no. DP305), and the quality was assessed by electrophoresis in 2 % agarose gels. Total RNA was extracted from the samples using a RNAprep Pure Plant Plus kit (TIANGEN, #Cat no. DP441), and RNA quality was checked by electrophoresis in 2 % agarose gels. A NanoDrop 2000c spectrophotometer (ThermoFisher, #Cat no. 11840461) was used to determine RNA concentration. Prior to sequencing library construction, the quality of the samples was assayed using an Agilent 2100 Bioanalyzer (Agilent Technologies, G2939BA), and the samples were quantified using a Qubit dsDNA HS assay kit (ThermoFisher, #Cat no. Q32851) or a Qubit RNA HS assay kit (ThermoFisher, #Cat no. Q32852). The mRNA was purified using Oligo $d(T)_{25}$ Dynabeads (ThermoFisher, #Cat no. 61002); all procedures were performed following the manufacturers' instructions.

2.5. Whole-genome bisulfite sequencing and data analysis

Lambda DNA was added to purified gDNA as an internal control to evaluate the subsequent C-to-T conversion efficiency. DNA was fragmented with a Bioruptor device (ThermoFisher, DS5300-0507), end repaired, ligated with methylated adapters, and DNA fragments 320 bp to 420 bp long were selected. The DNA was treated with bisulfite using an EZ DNA Methylation-Gold kit (Zymo Research, Cat No. D5005). The library was amplified using PCR and qualified by qPCR. The libraries were sequenced on the Illumina HiSeq X Ten platform in 150 PE mode; each library generated approximately 60 G (30×) data.

Based on the latest version of the Moso bamboo genome (Chromosome level Hi-C version) [23], index files were created using Bismark software with the bismark_genome_preparation command [24], and DNA 5mC methylation was recognized with the command: *bismark_methylation_extractor -p –no_overlap –comprehensive –report –bedGraph –CX_report –scaffolds –cytosine_report*. Differentially methylated regions

(DMRs) were defined as regions < 100 bp with differences in CG, CHG, and CHH methylation levels ≥ 0.4, 0.2, and 0.1, respectively. DMRs were detected using the R/Bioconductor package DMRcaller with default parameters [25].

2.6. Strand-specific RNA-seq, small RNA-seq, and data analysis

Strand-specific RNA-seq libraries were constructed from mRNA fragments and sequenced using the Illumina HiSeq platform. Reads were mapped to the Moso bamboo chromosome-level reference genome [23] using TopHat (v2.0.11) with the parameters *–read-mismatches 5 –read-gap-length 5 –read-edit-dist 5 -p 10 -r 50 -a 8*. Assembly was performed using Cufflinks (v2.1.1) with the following parameters: *-F 0.05 -A 0.01 -I 100000 –min-intron-length 30*. Differentially expressed genes (DEGs) were identified using edgeR from the R package with the criteria fold change (FC) > 2 with FDR < 0.05 [26].

Approximately 1.0 μg total RNA was used to prepare a small RNA library, which was sequenced on the Illumina HiSeq platform. The FASTX toolkit was used to trim the adaptor sequences with the command: *fastx_clipper -Q 33 -a CTGTAGGCACCATCAATCA -l 16 -d 0 -n -v -M 4*. Bowtie (v2.2.1) was used to align the reads to the reference genome with the command: *bowtie2 -k 20 –no-unal –no-hd –no-sq*. miRNAs were identified by aligning all small RNA reads to the miRBase 21 mature miRNA database (https://www.mirbase.org/), without allowing mismatches. The small RNA reads were counted and scaled to reads per million mapped reads (RPM).

3. Results

3.1. Morphological and cytological characteristics of the underground rhizome-root system in Moso bamboo

We collected bamboo rhizome lateral buds (LB) (Fig. 1A), flagellate rhizome tips (RT) (Fig. 1B), and roots growing from new shoots (RGFNS) (Fig. 1C) for analysis. The RT epidermal trichomes tended to range from sparse to dense from the top to the base (Fig. 1D), and the stomatal structure was clearly visible. The inner epidermis of LB had a well-defined outline, the outer epidermis was flat, the epidermal trichomes were dense, and the stomata were smaller (Fig. 1D). SAM cells underwent differentiation and developed into all types of tissues such as sheath leaves, pith tissues, and adventitious roots (Fig. 1E and F).

LB located near the rhizome groove had a compact and flattened structure (Fig. 1B). The LB was divided into different regions, including the proximal, middle, and distal region, based on their distance from the mother plant (Fig. 1A), which we referred to as LB_p, LB_m, and LB_d, respectively. The angles of divergence in the SAM varied (Fig. 1G): LB_p had the largest divergence angles, followed by LB_m and LB_d. We also detected a negative correlation between the SAM angle size and the distance to the mother plant (Fig. 1H), that is, the greater distance, the smaller the angle. Using the above materials, we explored the regulation of DNA methylation, gene expression, and small RNAs in the rhizome-root system of Moso bamboo.

3.2. Transcriptional analysis of different underground rhizome-root tissues in Moso bamboo

To quantify gene expression, we performed strand-specific transcriptome sequencing (RNA-seq) using five different tissues from the underground parts of the plant, including LB_p, LB_m, LB_d, RT, and RGFNS. According to Spearman correlation analysis, a clear distinction was detected among tissues, with good repeatability within the same tissue (Fig. 2A). LB shared greater similarity with RT and were distinguishable from RGFNS. Nonlinear dimensionality reduction (ISOmap) revealed similar trends (Fig. 2B). FPKM measurements indicated that overall, the gene expression levels were highest in RT, followed by LB and RGFNS (Fig. 2C). This result is consistent with the finding that RT exhibited rapid proliferation. RGFNS are mature and have completed their morphological development and primarily function in absorbing water and nutrients.

We calculated the correlation between DEGs among tissues, finding similar patterns of DEGs in all three regions of the LB (Fig. 2D). The gene expression profiles of RT, RGFNS, and LB tissues were significantly distinct, especially between LB and RGFNS, which is consistent with the results of cytological and morphological analysis (Fig. 1A) and overall transcriptome analysis (Fig. 2C). The number of DEGs between each pair of tissues is shown in Fig. 2E, with the highest count observed between LB and RGFNS (nearly 20,000), followed by that between LB and RT. The lowest number of DEGs was identified among different regions (proximal, middle, and distal) of LB, which is consistent with the clusters obtained by transcriptome analysis (Fig. 2A and B).

Heatmap cluster analysis separated the DEGs into six distinct groups (Fig. 2F). Highly expressed genes with tissue-specific expression were observed in the first (I), second (II), fourth (IV), and fifth (V) clusters, corresponding to RGFNS (I), LB (II, IV), and RT (V), respectively. The exclusive expression of genes in the LB might be required to maintain its state. Furthermore, the genes belonging to the third cluster are highly expressed in both LB and RT, whereas the genes in the sixth cluster are highly expressed in both RT and RGFNS. Genes in the same cluster might share similar functions, such as multipotent differentiation capacity in RT and LB and nutrient absorption in RT and RGFNS.

The top 20 enriched Gene Ontology (GO) terms among the highly expressed genes in LB, RGFNS, and RT are shown in Fig. S1. Genes involved in development, such as organ growth and reproductive structure development, were highly expressed in LB (Fig. S1A). Genes related to environmental responses, such as the regulation of defense responses and response to stimulus, were highly abundant in RGFNS (Fig. S1B). Genes associated with cell proliferation and differentiation were enriched in RT, such as genes involved in asymmetric cell division and the cell cycle (Fig. S1C). The distinct enrichment of genes in these three different tissues might be associated with the specific roles that LB, RGFNS, and RT play in the physiology of Moso bamboo.

3.3. Analysis of phytohormone-related gene clusters in different underground rhizome-root tissues of Moso bamboo

Phytohormones regulate lateral bud differentiation in Moso bamboo [27,28]. To explore whether phytohormones function in the growth and development of the rhizome-root system in Moso bamboo, we identified the phytohormones-associated DEGs (Table S1) and generated heatmaps with hierarchical clustering by Pearson correlation analysis (Fig. S2). IAA-related DEGs were roughly divided into seven categories (Fig. S2A); ABA-associated DEGs were classified into six categories (Fig. S2B); BR-related DEGs were divided into four categories (Fig. S2C); cytokinin (CTK)-related DEGs were roughly divided into five categories (Fig. S2D); and GA-related DEGs were divided into three categories (Fig. S2E). Notably, a larger proportion of IAA-, ABA-, BR- and CTK-related DEGs were downregulated in RGFNS but upregulated in RT, revealing the distinct regulation of IAA, ABA, BR, and CTK in RGFNS and RT. These results suggest that phytohormones play specific roles in regulating the development of the rhizome-root system of Moso bamboo.

We examined the motifs present in the 2 kb promoter regions of phytohormones-related genes as an indication of potential regulation by TCP-type transcription factors (Fig. S3A). We identified 67 expressed TCP-type transcription factor genes in tissues of the rhizome-root system. We then performed Spearman correlation analysis between these TCP-type transcription factors and 783 phytohormone-related genes, finding a high degree of correlation (Fig. S3B). These findings point to the potential regulation of these phytohormone-related genes by TCP-type transcription factors.

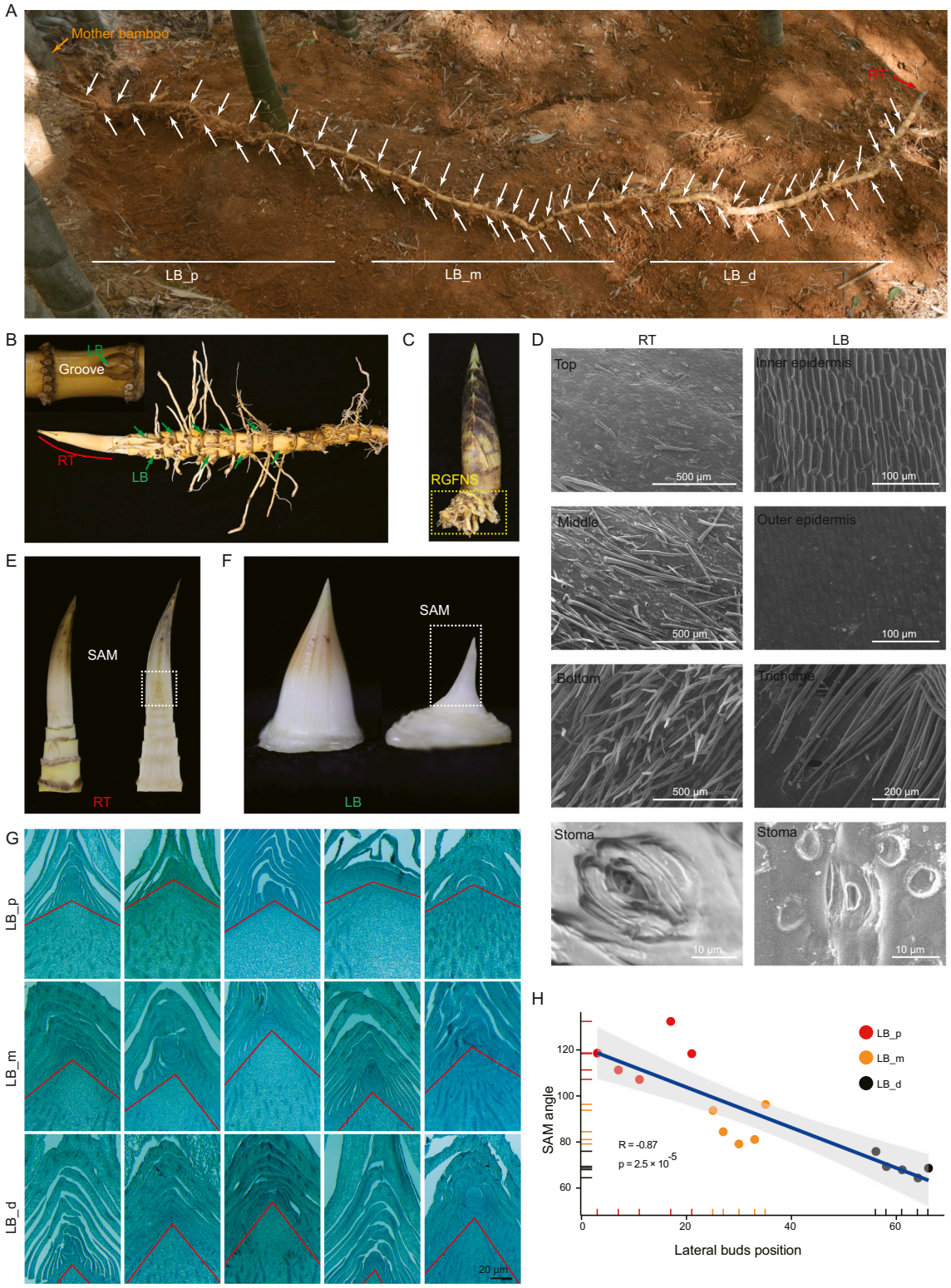

Fig. 1. The morphological and cytological characteristics of the underground rhizome-root system in Moso bamboo. A. The underground parts of bamboo. The white arrows indicate the lateral buds, which were divided into three distinct regions based on their distance from the mother plant: the proximal (LB_p), middle (LB_b), and distal (LB_d) regions. The orange arrow marks the location of the mother plant. B. Magnified view of the RT (indicated by a red curve) and LB (denoted by green arrows). C. Magnified view of roots growing from a new shoot (RGFNS, enclosed in a yellow box). D. Scanning electron microscopy of RT and LB. E. SAM of the RT (contained within the white box); F. The intact SAM (enclosed in a white box) after the hulling of LB; G. Paraffin sections of LB; pith angle is marked in red. H. The correlation between SAM angle and the distance from the mother plant. LB_p: proximal lateral buds, LB_m: middle lateral buds, LB_d: distal lateral buds. RT: The rhizome tip. LB: lateral buds. RGFNS: Roots growing from new shoots. SAM: shoot apical meristem.

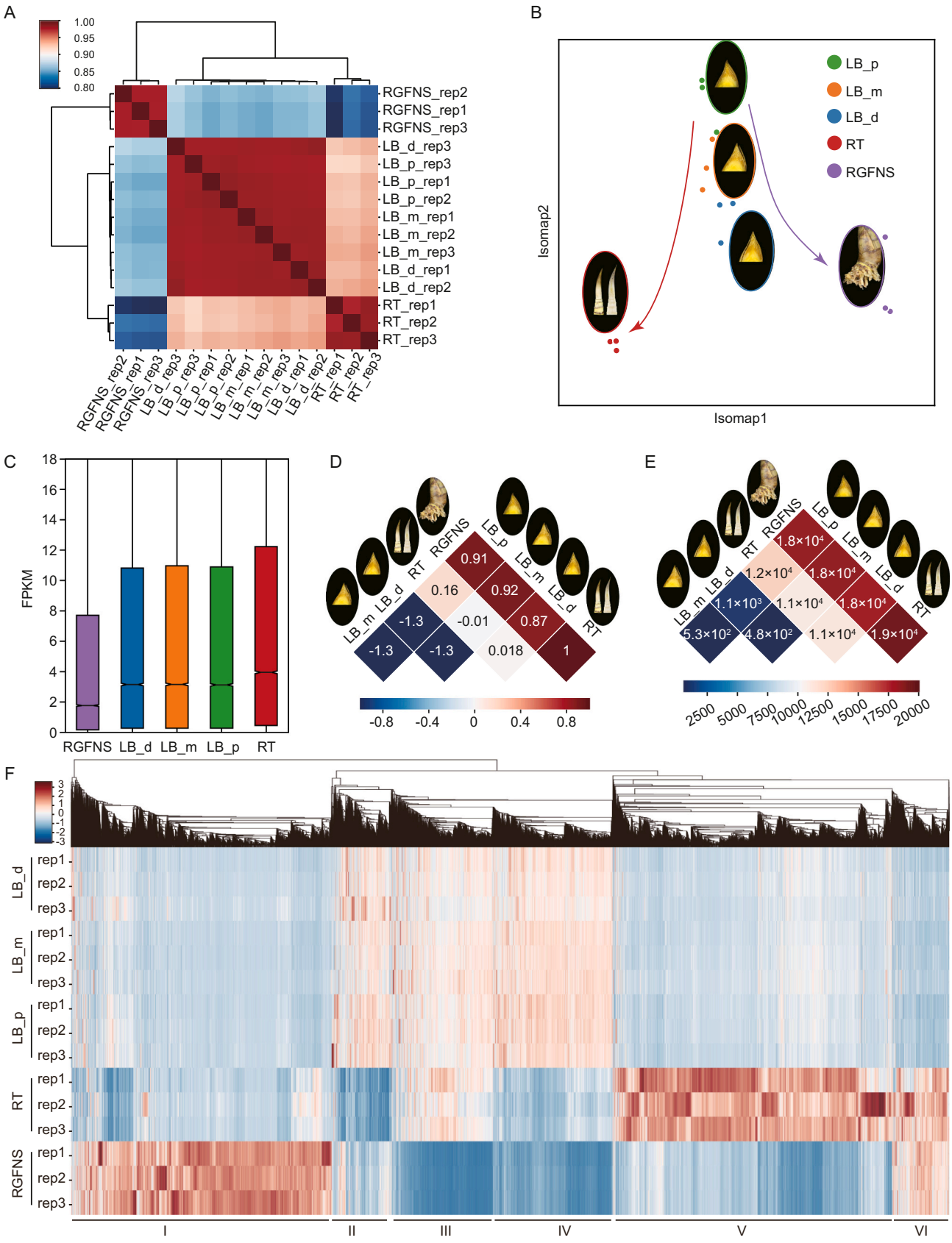

Fig. 2. Analyzing RNA-seq data from the rhizome-root system of Moso bamboo. A. Spearman correlation analysis. B. ISOmap dimensionality reduction analysis. C. Comparative analysis of gene expression. D. Heatmap of the correlation of differentially expressed genes (DEGs) across tissues. The values in the heatmap are represented as z-scores, which were calculated using the following formula: (Number of DEGs - Average number of DEGs)/Standard deviation. E. Heatmap of the number of DEGs among tissues. F. Cluster analysis of DEGs, which were clustered into six groups.

3.4. DNA methylation analysis of different underground rhizome-root tissues of Moso bamboo

DNA methylation is not evenly dispersed in plant genomes but is predominantly concentrated in repetitive regions, such as TEs, which can contribute to genome evolution [29,30]. Active TEs have the potential to affect the stability of the genome [31]. To evaluate the distribution of DNA methylation in TEs, we conducted whole-genome bisulfite sequencing (WGBS) of mCG, mCHG, and mCHH in these regions. Overall, we detected hypermethylated TE regions among tissues (Fig. 3A). High levels of mCG and mCHG methylation were detected in the TE regions among tissues, whereas they were stratified in the flanking regions (within ±1 kb) of transcription start sites (TSSs) and transcription termination site (TTSs). The mCHH levels in the flanking region showed little change, whereas there was obvious stratification in the transcribed regions of TEs ranging from 5 % to 30 %. A higher mCHH level was observed in LB than RGFNS and RT, especially in LB_d (Fig. 3A). These results suggest that mCHH is associated with the development of the rhizome-root system of Moso bamboo.

To explore the distribution of DNA methylation in TEs, we analyzed the four major types of TEs: DNA, LINE, LTR and SINE TEs. We observed the same trend of hypermethylation in the transcribed region and hypomethylation in the ±1 kb region of TSSs and TTSs (Fig. S4). The mCHH levels were significantly stratified by tissues; LB, especially in the distal side (LB_d), had the highest mCHH levels (Fig. S4). Among the four types of TEs, DNA and SINE TEs showed the most distinct patterns in the different underground root tissues of Moso bamboo (Fig. S4).

We previously showed that the mCHH levels in the TE regions of both leaves and floral organs of Moso bamboo at different physiological ages are approximately 8 % [32]. In the current study, the levels of mCHH of TEs were relatively high in underground tissues, especially LB, with levels as high as 30 % in LB_d (Fig. 3A). To further explore the high mCHH levels in different underground tissues of Moso bamboo, we calculated the DNA methylation ratios of all nine CHH contexts (where H is any base except G) (Fig. S5). The DNA methylation levels varied among CHH contexts, with relatively high mCAA, mCAT, mCAC, and mCTA levels, especially in LB_d, with a ratio > 10 % (Fig. S5). The level of mCCC methylation was relatively low (Fig. S5). The level of mCTA

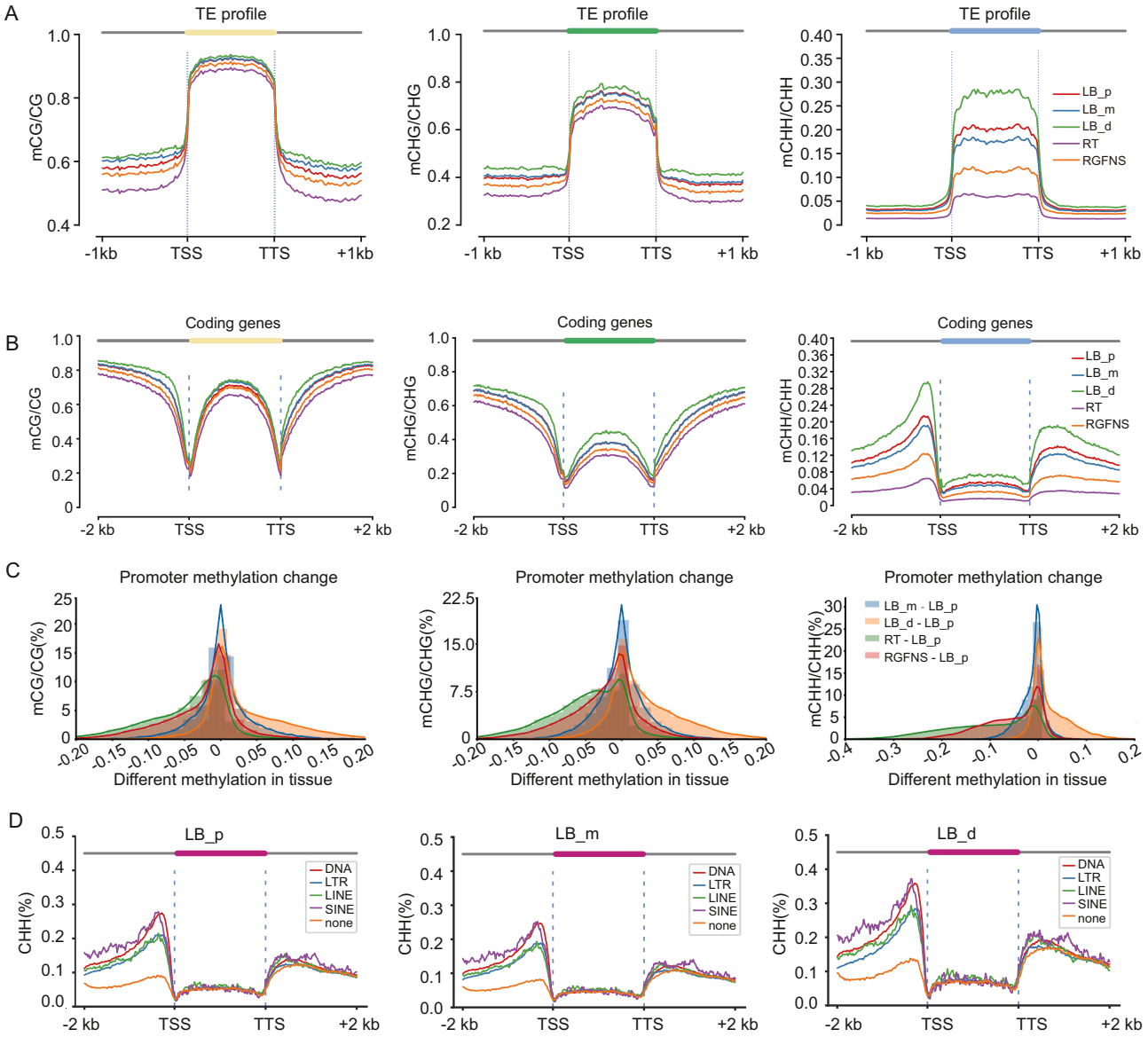

Fig. 3. The distribution patterns of mCG, mCHG, and mCHH. A. Distribution patterns in TEs. B. Distribution patterns in protein-encoding genes. C. Distribution of methylation profiles in promoters. D. CHH methylation levels in protein-encoding genes including TEs (DNA, LTR, LINE, and SINE). None indicates genes without any TEs in the gene body or within 2 kb of the TSS/TTS.

methylation was the highest, reaching 35 % in LB_d (Fig. S6), whereas the level in RT was approximately 11 %. These results suggest that mCHH regulates the development of root tissues of Moso bamboo via the hypermethylation of specific contexts.

We then examined the DNA methylation patterns of all annotated protein-encoding genes. mCG and mCHG showed hypermethylation at approximately ±2 kb of TSSs and TTSs but hypomethylation at TTSs and TSSs (Fig. 3B). Notably, the profile of mCHH is quite different: the gene body was hypomethylated, and the regions ±2 kb of TSSs and TTSs were hypermethylated. The mCHH levels were significantly stratified in different tissues, and LB showed a significantly higher methylation level than RT and RGFNS (Fig. 3B). The ratio of mCHH of protein-encoding genes in aboveground tissues was previously shown to range from 2 % to 6 % [32]. Similarly, in the current study, the mCHH levels of protein-encoding genes in underground root tissues ranged from 3 % to 30 %, and the mCHH levels of LB were >8 % (Fig. 3B). We also compared the types of methylation among tissues. The mCHH levels in the promoter regions of genes were as high as 30 %, i.e., much higher than that of mCG (25 %) and mCHG (22 %), suggesting that mCHH could play a significant regulatory role in the rhizome-root system of Moso bamboo (Fig. 3C). Moreover, LB exhibited the most significant variation in mCHH levels compared to other tissues.

To investigate the high abundance of CHH in LB tissues, we identified the four major categories of TEs (LTR, LINE, SINE, and DNA) around protein-encoding genes. We subsequently compared the distribution of CHH contexts in the four major categories of TEs around protein-encoding genes vs. protein-encoding genes without TEs in LB tissues (Fig. 3D). Compared to CHH in protein-encoding genes without TEs, protein-encoding genes containing the four major categories of TEs showed a higher proportion of methylation in the CHH context, which was observed within ±2 kb of TSSs and TTSs, particularly in the −2 kb region of TSSs. The dissimilarity in mCHH levels might be linked to the diverse angle sizes of SAMs in LB tissues.

In addition, we investigated the ABA-, IAA-, BR- and CTK-related genes that exhibited CG, CHG, and CHH DMRs simultaneously. We identified four ABA-related genes (PH02Gene14516, PH02Gene24143, PH02Gene30539, and PH02Gene31022), one IAA-related gene (PH02Gene14676), and one CTK-related gene (PH02Gene30734) that

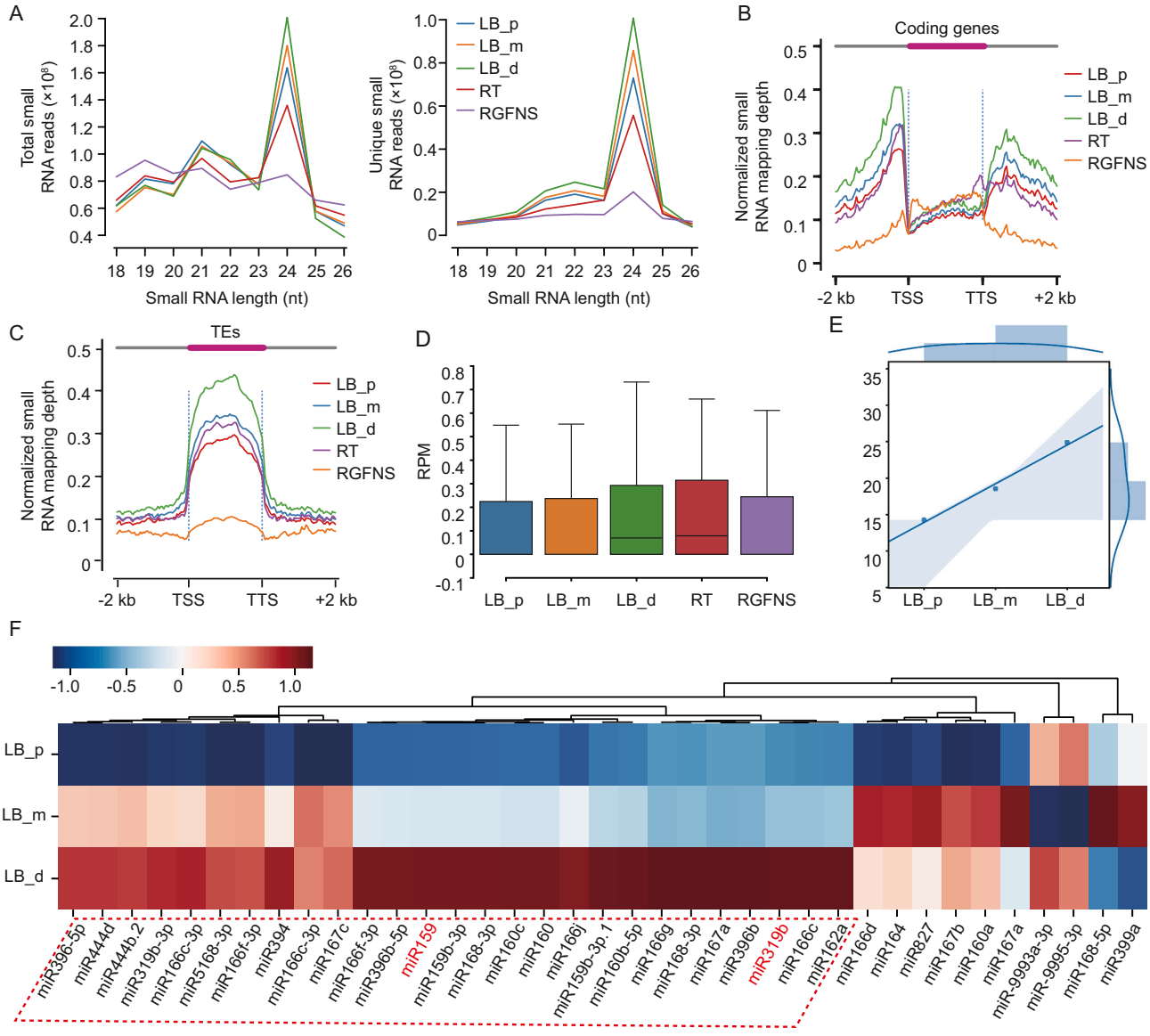

Fig. 4. Analysis of small RNAs. A. Read distribution of small RNA ranging from 18 to 26 nt in underground root tissues of Moso bamboo. B. Distribution of 24 nt small RNAs in protein-encoding genes across different tissues. C. Distribution patterns of 24 nt small RNAs in TEs. D. Box plots depicting the abundance of known miRNAs across various tissues. E. Correlation analysis of miRNA abundance and the distance from the mother plant in LB. F. Cluster analysis of miRNAs in LB.

displayed DMRs in all three categories (Fig. S3C–E). These genes exhibited gradual changes in expression across various tissues of the rhizome-root system (Fig. S3C–E).

3.5. Small RNA analysis of different underground rhizome-root tissues of Moso bamboo

Small RNAs, which are tightly linked to DNA methylation, are also involved in epigenetic regulation [33,34]. Hence, we tallied the overall count of distinct and clean small RNA reads ranging from 18 to 26 nucleotides; 24 nt small RNA reads were the most abundant (Fig. 4A). Among the unique small RNA reads, 24 nt sequences were the most abundant in LB and least abundant in RGFNS, exhibiting a similar trend of stratification with mCHH.

In view of the close regulatory relationship between small RNAs and DNA methylation [35], we analyzed the distribution of small RNAs in both protein-encoding genes (Fig. 4B) and TE regions (Fig. 4C). 24 nt small RNAs were present at low levels in the gene body (from the TSS to TTS), with no obvious stratification among different tissues (Fig. 4B). In the region around ±2 kb of TSSs and TTSs, RT and LB had a similar distribution pattern, whereas RGFNS showed lower levels of these small RNAs (Fig. 4B). Among TEs, 24 nt small RNAs were mainly distributed in TE regions (from the TSS to TTS), with stratification in different tissues (Fig. 4C). A similar distribution pattern in TEs was observed for both 24 nt small RNAs and mCHH (Fig. 3A), suggesting that small RNAs are associated with mCHH.

As miRNAs are involved in regulating gene expression [36], we investigated whether miRNAs take part in the development of the root system of Moso bamboo. We calculated the expression levels of known miRNAs from miRBase and determined that the abundance of miRNAs was highest in RT (Fig. 4D). In LB tissue, there appeared to be a slight increase in miRNA abundance with increasing distance from the mother plant (LB_p < LB_m < LB_d) (Fig. 4E).

To identify the specific miRNAs that function in LB development, we conducted hierarchical clustering based on z-scores. Approximately 90 % (~27) of the 37 miRNAs exhibited an increase in expression (indicated by a dotted line) as the distance from the mother plant increased (Fig. 4F). MYB transcription factors, which perform a variety of functions, are targeted by miR159 and miR319; these two miRNAs are expressed at high levels in LB_d [37,38].

3.6. Association analysis of DNA methylation and gene expression in underground rhizome-root tissues of Moso bamboo

To investigate the epigenetic regulation of gene expression, we performed correlation analysis to assess the effect of DNA methylation on gene expression (Fig. 5 and Fig. S7). We observed a correlation between gene expression and mCG methylation at protein-encoding gene body regions. For genes without any detected expression, we observed high mCG levels in both the gene body and regions ±2 kb from the TSS and TTS. Similar results were obtained for mCHG. Regarding mCHH methylation, hypermethylation of the promoter region (+2 kb of the TSS) was positively correlated with high gene expression levels (Fig. 5 and Fig. S7). The level of mCHH methylation was highest in LB, followed

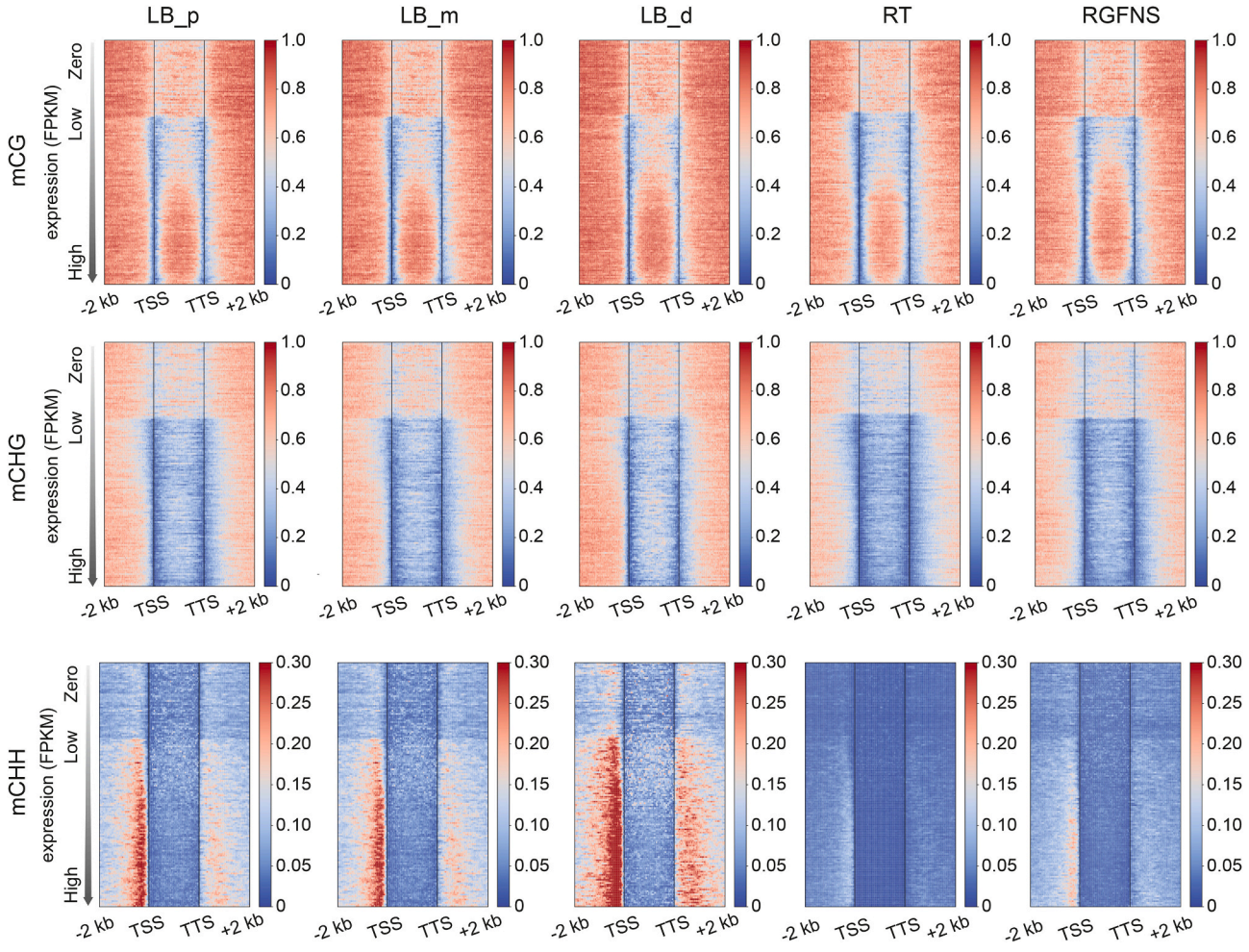

Fig. 5. Correlation analysis of DNA methylation and gene expression levels in underground rhizome-root tissues of Moso bamboo.

by RGFNS and RT, as also shown in Fig. 3. By contrast, we observed low mCHH levels in the both gene body and regions ±2 kb from the TSS and TTS for genes without any detected expression (Fig. 5 and Fig. S7).

3.7. Association analysis of DNA methylation and gene expression in underground rhizome-root tissues of Moso bamboo

To further investigate the relationship between DNA methylation and gene expression, we focused on specific DEGs. Since specific transcription factors are known to play a crucial role in regulating gene expression, we analyzed the motifs around the promoter regions of the DEGs, finding that a significant proportion of DEGs could be regulated by C2H2-type transcription factors (Fig. 6A). DEGs associated with C2H2-type transcription factors could be divided into four distinct groups based on gene expression patterns (Fig. 6B). DEGs belonging to Group I exhibited relatively high expression levels in LB and RT, whereas group II, III, and IV DEGs showed elevated expression specifically in RT, LB, and RGFNS, respectively. The tissue-specific expression patterns of these genes point to their involvement in the development of Moso bamboo.

C2H2-type transcription factors have a well-characterized binding motif, A**CG**A**CAA**A (Fig. 6C), which is a potential motif for mCG and mCHH methylation. Therefore, we searched for differences in mCHH methylation in C2H2-type motifs around the promoter regions (+2 kb of the TSS) of DEGs. We observed differences in mCHH levels via pairwise comparisons of various underground rhizome tissues of Moso bamboo. In particular, a significant reduction in mCHH levels of C2H2-type motifs was observed in RT and RGFNS compared to LB_p (Fig. 6D). The differences in mCHH methylation may influence the binding of the corresponding C2H2 transcription factors, leading to variations in the expression of target genes across different underground rhizome tissues of Moso bamboo.

4. Discussion

In this study, we focused on the underground rhizome-root system, which is essential for the rapid growth of Moso bamboo. Initially, we examined the morphological and cytological features of the underground tissues. Notably, a negative correlation was observed between the angle of the SAM and the distance from the mother plant in LB tissue (Figs. 1H and 7). A previous study of the SAMs of awakening buds showed that the diameter of the bamboo culm (thickening growth) is dependent on the size and shape of the SAM. For example, an enlarged SAM produces a stem characterized by a narrow pith cavity and thick culm wall [39]. Since Moso bamboo is a scattered species, it is commonly believed that the distal lateral buds (LB_d), situated further away from the mother plant, have a higher propensity to differentiate into RT, whereas the proximal lateral buds (LB_p), located closer to the

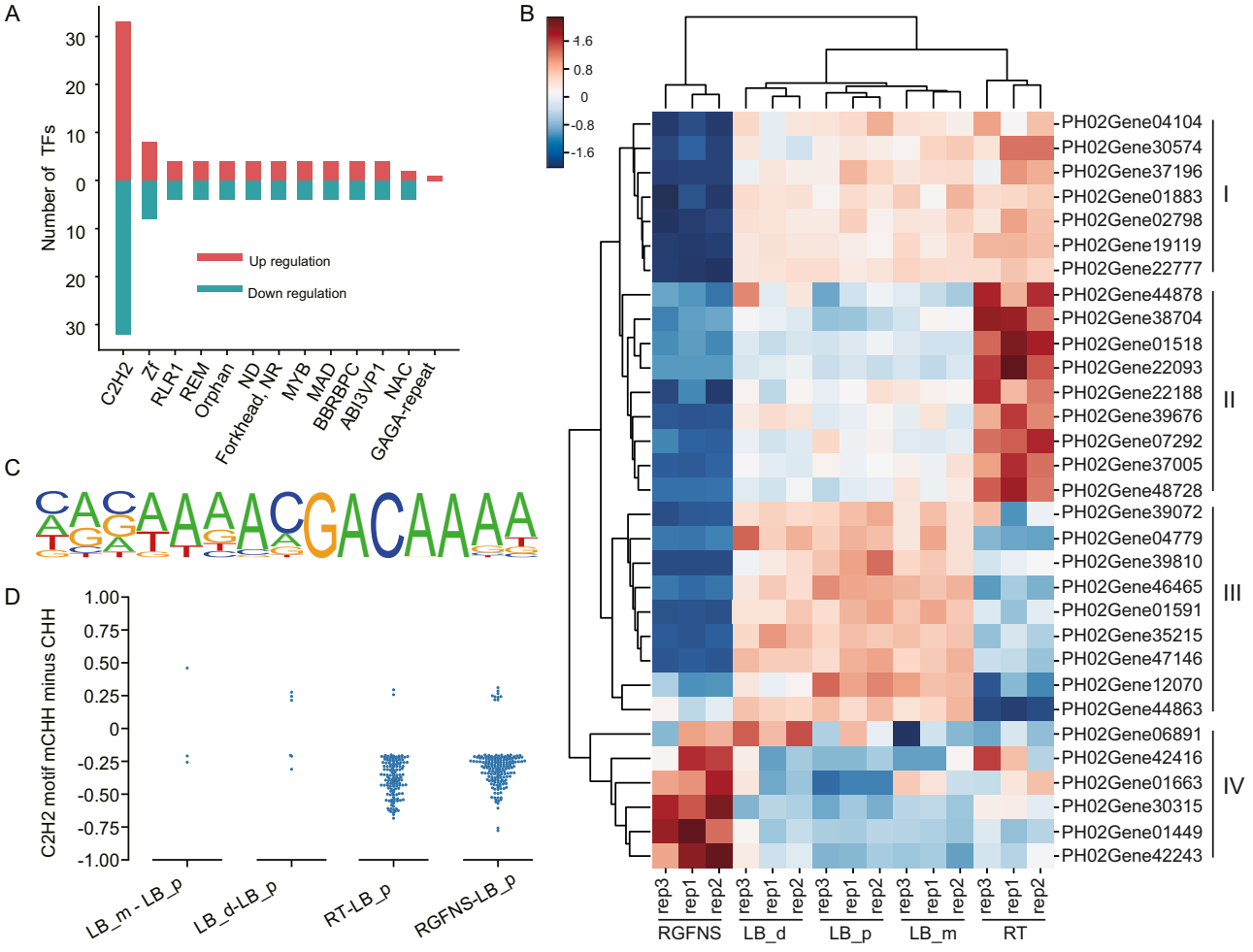

Fig. 6. Differential methylation levels of C2H2 motifs in the promoters of DEGs. A. Promoter motif analysis of DEGs. Red represents the count of transcription factors corresponding to the promoters (+2 kb of TSS) of upregulated genes (FC > 2), while blue indicates the count of transcription factors corresponding to downregulated genes (FC < 0.5). B. Expression profiles of DEGs containing binding motifs of C2H2-transcription factors in underground rhizome-root tissues. C. Characteristics of motif sequences in C2H2-type transcription factors. D. Differential mCHH methylation levels in C2H2 motifs compared to LB_p.

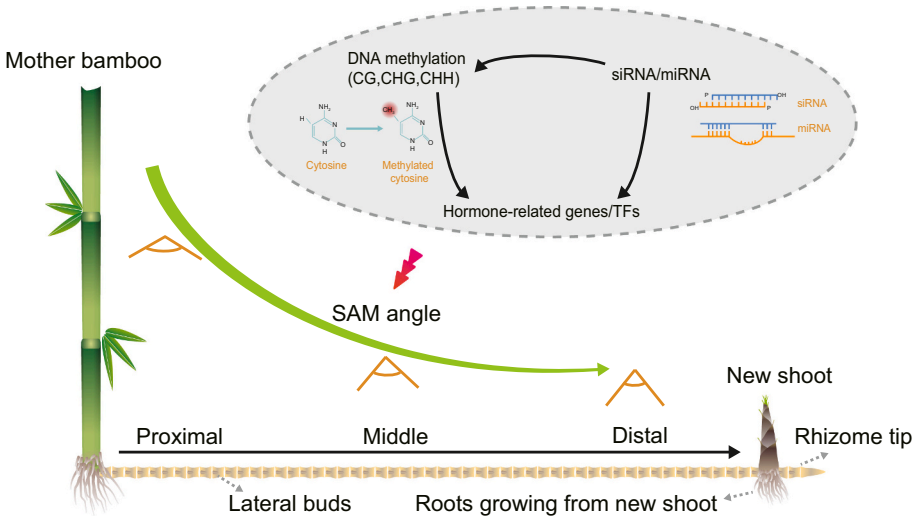

Fig. 7. Model illustrating the key findings of this study. The circle consists of three components: DNA methylation, small RNA, and targeted genes (phytohormone-related genes and transcription factor genes). We propose that phytohormone-related and transcription factor genes are regulated by both DNA methylation and small RNAs, which could be associated with the SAM angles within lateral buds.

mother plant, are more likely to develop into new shoots [16,40]. We propose that the different angles of the SAM in buds are associated with the different directions of differentiation.

To gain insight into the mechanisms underlying the rapid growth of Moso bamboo, we generated whole-genome single-base resolution DNA methylome maps of the underground rhizome-root system of this plant (Fig. S8). The hypermethylation of TEs, notably in the mCG and mCHG contexts, has been observed in both angiosperms and gymnosperms [41–44]; we observed such a phenomenon in Moso bamboo (Fig. 3A). The methylation levels (including mCG, mCHG, and mCHH) of protein-encoding genes were significantly higher in LB than in RGFNS and RT (Fig. 3A and B). In particular, the distribution of mCHH in underground root tissues of Moso bamboo was distinctive, occurring both within protein-encoding genes and TEs. Surprisingly, the mCHH levels in the promoter and gene body regions of LB_d, including both TEs and protein-encoding genes, were as high as 30 %. This is significantly higher than what was previously reported in aboveground tissues of Moso bamboo, ranging from 2 % to 6 % [32]. Compared to other species, such as *Arabidopsis thaliana* seedlings (protein-encoding genes < 3 %, TEs < 20 %) [45], the SAM of *Oryza sativa* (protein-encoding genes < 10 %, TE regions < 16 %) [46], the forest tree Norway spruce (*Picea abies*) (protein-encoding genes and TEs < 3 %) [47], and *Populus trichocarpa* (protein-encoding genes < 5 %) [48], the mCHH levels in LB_d (protein-encoding genes ~30 % and TEs ~30 %) were also notably elevated. The greatest contributors to the high mCHH levels in Moso bamboo were mCAA, mCAT, mCAC, and mCTA methylation.

DRM1 and DRM2, which are plant counterparts of mammalian DNMT3, play crucial roles in CHH methylation [49]. Therefore, we investigated the expression levels of *DRM1/2* in various tissues. *DRM1/2* were expressed at relatively high levels in RT, followed by LB and RGFNS. No significant differences in *DRM1/2* expression were observed among LB tissues (Fig. S9), suggesting that the major cause of the observed differences in DNA methylation might be associated with small RNAs.

Apart from the higher methylation levels in LB_d, we also discovered a greater abundance of miRNAs in LB_d (Fig. 4E). Taken together, these findings suggest that epigenetic regulation plays a crucial role in the development of Moso bamboo (Fig. 7). Notably, two miRNAs that target MYB genes, miR159b and miR319, were highly expressed in LB_d. This observation is in line with the finding that the MYB family is involved in regulating lateral bud development [50,51].

We then conducted integrated analysis of gene expression and small RNAs to obtain a comprehensive view of the epigenetic regulation of the rhizome-root system. In Moso bamboo, we observed high mCG and mCHG methylation levels around protein-encoding genes without any detected expression (Fig. 5), suggesting that high levels of mCG and mCHG suppress gene expression, which is consistent with previous findings [52]. For genes with detected expression, we determined that DNA methylation in gene body regions promotes gene transcription, which is consistent with previous findings, such as *ROS1* in *Arabidopsis* and various genes in tomato [53], as well as species such as cassava [54], soybean [55], and poplar [56]. Importantly, we observed a significant increase in mCHH methylation levels in promoter regions in LB with increasing gene expression, especially near TSSs and TTSs (Fig. 5). These findings suggest that high levels of mCHH promote gene expression in LB, indicating that mCHH might regulate the development of the underground rhizome-root system in Moso bamboo by affecting gene expression.

We propose that genes, including phytohormones-related genes and transcription factor genes, are regulated by both DNA methylation and small RNAs. Consequently, these regulatory mechanisms can affect the development of various underground rhizome-root tissues in Moso bamboo, as indicated by the variations in the SAM angles within the LB (Fig. 7). In summary, our study represents the first attempt to elucidate the regulatory relationship between DNA methylation and the rapid growth of Moso bamboo from its underground rhizome-root tissues. Our findings provide a basis for further research on the underlying mechanisms driving the rapid growth of this species.

Supplementary data to this article can be found online at https://doi.org/10.1016/j.ijbiomac.2023.125921.

CRediT authorship contribution statement

HZ, JG, and LG conceived and designed the research. FX, LW, BW, PG, KC, and LZ performed experiments. ZZ, FX, and HZ performed bioinformatics. FX, HZ, and LG wrote the manuscript.

Declaration of competing interest

The authors declare that they have no competing interests or personal relationships that could have appeared to influence the work reported in this paper.

Data availability

Raw sequencing data are available in NCBI under accession number PRJNA914504.

Acknowledgements

We thank Yangyang Zhang from the College of Forestry of FAFU for his kind support in sample collection. Feihu Xi personally thanks his parents and uncle for their kind caring and listening during his Ph.D.

Funding

This research was supported by the National Key Research and Development Program of China (2021YFD2200505), the National Natural Science Foundation of China (grant no. 31971734), the Natural Science Foundation of Fujian Province (2021J02027), the Distinguished Young Scholar Program of Fujian Agriculture and Forestry University (xjq202017), the Fujian Provincial Department of Science and Technology (2021L3017), the Fujian Provincial Department of Forestry (ZMGG-0704), and the Forestry Peak Discipline Construction Project of Fujian Agriculture and Forestry University (72202200205).

References

[1] Q. Wei, L. Guo, C. Jiao, Z. Fei, M. Chen, J. Cao, Y. Ding, Q. Yuan, Characterization of the developmental dynamics of the elongation of a bamboo internode during the fast growth stage, Tree Physiol. 39 (7) (2019) 1201–1214.
[2] L. Li, Z. Cheng, Y. Ma, Q. Bai, X. Li, Z. Cao, Z. Wu, J. Gao, The association of hormone signalling genes, transcription and changes in shoot anatomy during moso bamboo growth, Plant Biotechnol. J. 16 (1) (2018) 72–85.
[3] J. Luo, R. Liu, S. Zhang, C. Lian, F. Yang, B. Fei, Comparative culm anatomy of metaxylem vessel pits in three different types of bamboo rhizome, IAWA J. 41 (2) (2020) 141–158.
[4] K. Wang, H. Peng, E. Lin, Q. Jin, X. Hua, S. Yao, H. Bian, N. Han, J. Pan, J. Wang, Identification of genes related to the development of bamboo rhizome bud, J. Exp. Bot. 61 (2) (2010) 551–561.
[5] M. Chen, L. Guo, M. Ramakrishnan, Z. Fei, K.K. Vinod, Y. Ding, C. Jiao, Z. Gao, R. Zha, C. Wang, Z. Gao, F. Yu, G. Ren, Q. Wei, Rapid growth of Moso bamboo (Phyllostachys edulis): cellular roadmaps, transcriptome dynamics, and environmental factors, Plant Cell 34 (10) (2022) 3577–3610.
[6] L. Guo, C. Wang, J. Chen, Y. Ju, F. Yu, C. Jiao, Z. Fei, Y. Ding, Q. Wei, Cellular differentiation, hormonal gradient, and molecular alternation between the division zone and the elongation zone of bamboo internodes, Physiol. Plant. 174 (5) (2022), e13774.
[7] Z. Gao, L. Guo, M. Ramakrishnan, Y. Xiang, C. Jiao, J. Jiang, K.K. Vinod, Z. Fei, F. Que, Y. Ding, F. Yu, T. Chen, Q. Wei, Cellular and molecular characterizations of the irregular internode division zone formation of a slow-growing bamboo variant, Tree Physiol. 42 (3) (2022) 570–584.
[8] M. Chen, Y. Ju, Z. Ahmad, Z. Yin, Y. Ding, F. Que, J. Yan, J. Chu, Q. Wei, Multi-analysis of sheath senescence provides new insights into bamboo shoot development at the fast growth stage, Tree Physiol. 41 (3) (2020) 491–507.
[9] K. Nagai, Y. Mori, S. Ishikawa, T. Furuta, R. Gamuyao, Y. Niimi, T. Hobo, M. Fukuda, M. Kojima, Y. Takebayashi, A. Fukushima, Y. Himuro, M. Kobayashi, W. Ackley, H. Hisano, K. Sato, A. Yoshida, J. Wu, H. Sakakibara, Y. Sato, H. Tsuji, T. Akagi, M. Ashikari, Antagonistic regulation of the gibberellic acid response during stem growth in rice, Nature 584 (7819) (2020) 109–114.
[10] H. Zhang, H. Wang, Q. Zhu, Y. Gao, H. Wang, L. Zhao, Y. Wang, F. Xi, W. Wang, Y. Yang, C. Lin, L. Gu, Transcriptome characterization of moso bamboo (Phyllostachys edulis) seedlings in response to exogenous gibberellin applications, BMC Plant Biol. 18 (1) (2018) 125.
[11] Y. Li, D. Zhang, S. Zhang, Y. Lou, X. An, Z. Jiang, Z. Gao, Transcriptome and miRNAome analysis reveals components regulating tissue differentiation of bamboo shoots, Plant Physiol. 188 (4) (2022) 2182–2198.
[12] M. Ramakrishnan, K. Yrjälä, K.K. Vinod, A. Sharma, J. Cho, V. Satheesh, M. Zhou, Genetics and genomics of moso bamboo (Phyllostachys edulis): current status, future challenges, and biotechnological opportunities toward a sustainable bamboo industry, Food Energy Secur. 9 (4) (2020), e229.
[13] G. McIntyre, Influence of nitrogen nutrition on bud and Rhizome development in Agropyron repens L. Beauv, Nature 203 (4949) (1964) 1084–1085.
[14] G.I. McIntyre, Apical dominance in the rhizome of Agropyron repens: the influence of water stress on bud activity, Can. J. Bot. 54 (23) (1976) 2747–2754.
[15] R. Leakey, R. Chancellor, D. Vince-Prue, Regeneration from rhizome fragments of Agropyron repens: I. The seasonality of shoot growth and rhizome reserves in single-node fragments, Ann. Appl. Biol. 87 (3) (1977) 423–431.
[16] Y. Shou, Y. Zhu, Y. Ding, Transcriptome analysis of lateral buds from Phyllostachys edulis rhizome during germination and early shoot stages, BMC Plant Biol. 20 (2020) 1–18.
[17] P. Gallusci, Z. Dai, M. Génard, A. Gauffretau, N. Leblanc-Fournier, C. Richard-Molard, D. Vile, S. Brunel-Muguet, Epigenetics for plant improvement: current knowledge and modeling avenues, Trends Plant Sci. 22 (7) (2017) 610–623.
[18] R.A. Rapp, J.F. Wendel, Epigenetics and plant evolution, New Phytol. 168 (1) (2005) 81–91.
[19] Z. Zhang, H. Wang, Y. Wang, F. Xi, H. Wang, M.V. Kohnen, P. Gao, W. Wei, K. Chen, X. Liu, Whole-genome characterization of chronological age-associated changes in methylome and circular RNAs in moso bamboo (Phyllostachys edulis) from vegetative to floral growth, Plant J. 106 (2) (2021) 435–453.
[20] S.A. Simon, B.C. Meyers, Small RNA-mediated epigenetic modifications in plants, Curr. Opin. Plant Biol. 14 (2) (2011) 148–155.
[21] L. Duempelmann, M. Skribbe, M. Bühler, Small RNAs in the transgenerational inheritance of epigenetic information, Trends Genet. 36 (3) (2020) 203–214.
[22] T.J. Collins, ImageJ for microscopy, Biotechniques 43 (S1) (2007) S25–S30.
[23] H. Zhao, Z. Gao, L. Wang, J. Wang, S. Wang, B. Fei, C. Chen, C. Shi, X. Liu, H. Zhang, Y. Lou, L. Chen, H. Sun, X. Zhou, S. Wang, C. Zhang, H. Xu, L. Li, Y. Yang, Y. Wei, W. Yang, Q. Gao, H. Yang, S. Zhao, Z. Jiang, Chromosome-level reference genome and alternative splicing atlas of moso bamboo (Phyllostachys edulis), Gigascience 7 (10) (2018).
[24] H. Lee, Analysis of bisulfite sequencing data using Bismark and DMRcaller to identify differentially methylated regions, Methods Mol. Biol. 2443 (2022) 451–463.
[25] M. Catoni, J.M. Tsang, A.P. Greco, N.R. Zabet, DMRcaller: a versatile R/Bioconductor package for detection and visualization of differentially methylated regions in CpG and non-CpG contexts, Nucleic Acids Res. 46 (19) (2018), e114.
[26] M.D. Robinson, D.J. McCarthy, G.K. Smyth, edgeR: a Bioconductor package for differential expression analysis of digital gene expression data, Bioinformatics 26 (1) (2010) 139–140.
[27] R. Gamuyao, K. Nagai, M. Ayano, Y. Mori, A. Minami, M. Kojima, T. Suzuki, H. Sakakibara, T. Higashiyama, M. Ashikari, S. Reuscher, Hormone distribution and transcriptome profiles in bamboo shoots provide insights on bamboo stem emergence and growth, Plant Cell Physiol. 58 (4) (2017) 702–716.
[28] J. Zhao, P. Gao, C. Li, X. Lin, X. Guo, S. Liu, PhePEBP family genes regulated by plant hormones and drought are associated with the activation of lateral buds and seedling growth in Phyllostachys edulis, Tree Physiol. 39 (8) (2019) 1387–1404.
[29] X. Zhang, J. Yazaki, A. Sundaresan, S. Cokus, S.W.-L. Chan, H. Chen, I. R. Henderson, P. Shinn, M. Pellegrini, S.E. Jacobsen, Genome-wide high-resolution mapping and functional analysis of DNA methylation in Arabidopsis, Cell 126 (6) (2006) 1189–1201.
[30] X.-J. He, T. Chen, J.-K. Zhu, Regulation and function of DNA methylation in plants and animals, Cell Res. 21 (3) (2011) 442–465.
[31] R.K. Slotkin, R. Martienssen, Transposable elements and the epigenetic regulation of the genome, Nat. Rev. Genet. 8 (4) (2007) 272–285.
[32] Z. Zhang, H. Wang, Y. Wang, F. Xi, H. Wang, M.V. Kohnen, P. Gao, W. Wei, K. Chen, X. Liu, Whole-genome characterization of chronological age-associated changes in methylome and circular RNAs in moso bamboo (Phyllostachys edulis) from vegetative to floral growth, Plant J. 106 (2) (2021) 435–453.
[33] M.G. Lewsey, T.J. Hardcastle, C.W. Melnyk, A. Molnar, A. Valli, M.A. Urich, J. R. Nery, D.C. Baulcombe, J.R. Ecker, Mobile small RNAs regulate genome-wide DNA methylation, Proc. Natl. Acad. Sci. U. S. A. 113 (6) (2016) E801–E810.
[34] J. Zhai, J. Liu, B. Liu, P. Li, B.C. Meyers, X. Chen, X. Cao, Small RNA-directed epigenetic natural variation in Arabidopsis thaliana, PLoS Genet. 4 (4) (2008), e1000056.
[35] M. Tamiru, T.J. Hardcastle, M.G. Lewsey, Regulation of genome-wide DNA methylation by mobile small RNAs, New Phytol. 217 (2) (2018) 540–546.
[36] M.W. Jones-Rhoades, D.P. Bartel, B. Bartel, MicroRNAs and their regulatory roles in plants, Annu. Rev. Plant Biol. 57 (2006) 19–53.
[37] X. Wang, Y. Niu, Y. Zheng, Multiple functions of MYB transcription factors in abiotic stress responses, Int. J. Mol. Sci. 22 (11) (2021).
[38] C. Dubos, R. Stracke, E. Grotewold, B. Weisshaar, C. Martin, L. Lepiniec, MYB transcription factors in Arabidopsis, Trends Plant Sci. 15 (10) (2010) 573–581.
[39] Y. Wang, X. Sun, Y. Ding, Z. Fei, C. Jiao, M. Fan, B. Yao, P. Xin, J. Chu, Q. Wei, Cellular and molecular characterization of a thick-walled variant reveal a pivotal role of shoot apical meristem in transverse development of bamboo culm, J. Exp. Bot. 70 (15) (2019) 3911–3926.
[40] L. Rui, H.J. During, M.J. Werger, Z.C. Zhong, Positioning of new shoots relative to adult shoots in groves of giant bamboo, *Phyllostachys pubescens*, Flora 193 (3) (1998) 315–321.
[41] S. Feng, S.J. Cokus, X. Zhang, P.-Y. Chen, M. Bostick, M.G. Goll, J. Hetzel, J. Jain, S. H. Strauss, M.E. Halpern, Conservation and divergence of methylation patterning in plants and animals, Proc. Natl. Acad. Sci. 107 (19) (2010) 8689–8694.
[42] A. Zemach, I.E. McDaniel, P. Silva, D. Zilberman, Genome-wide evolutionary analysis of eukaryotic DNA methylation, Science 328 (5980) (2010) 916–919.
[43] C.E. Niederhuth, A.J. Bewick, L. Ji, M.S. Alabady, K.D. Kim, Q. Li, N.A. Rohr, A. Rambani, J.M. Burke, J.A. Udall, Widespread natural variation of DNA methylation within angiosperms, Genome Biol. 17 (1) (2016) 1–19.
[44] D. Lang, K.K. Ullrich, F. Murat, J. Fuchs, J. Jenkins, F.B. Haas, M. Piednoel, H. Gundlach, M. Van Bel, R. Meyberg, The Physcomitrella patens chromosome-scale assembly reveals moss genome structure and evolution, Plant J. 93 (3) (2018) 515–533.
[45] T. Ito, Y. Tarutani, T.K. To, M. Kassam, E. Duvernois-Berthet, S. Cortijo, K. Takashima, H. Saze, A. Toyoda, A. Fujiyama, Genome-wide negative feedback drives transgenerational DNA methylation dynamics in Arabidopsis, PLoS Genet. 11 (4) (2015), e1005154.

[46] A. Higo, N. Saihara, F. Miura, Y. Higashi, M. Yamada, S. Tamaki, T. Ito, Y. Tarutani, T. Sakamoto, M. Fujiwara, DNA methylation is reconfigured at the onset of reproduction in rice shoot apical meristem, Nat. Commun. 11 (1) (2020) 4079.
[47] I. Ausin, S. Feng, C. Yu, W. Liu, H.Y. Kuo, E.L. Jacobsen, J. Zhai, J. Gallego-Bartolome, L. Wang, U. Egertsdotter, N.R. Street, S.E. Jacobsen, H. Wang, DNA methylome of the 20-gigabase Norway spruce genome, Proc. Natl. Acad. Sci. U. S. A. 113 (50) (2016) E8106–E8113.
[48] S. Feng, S.J. Cokus, X. Zhang, P.Y. Chen, M. Bostick, M.G. Goll, J. Hetzel, J. Jain, S. H. Strauss, M.E. Halpern, C. Ukomadu, K.C. Sadler, S. Pradhan, M. Pellegrini, S. E. Jacobsen, Conservation and divergence of methylation patterning in plants and animals, Proc. Natl. Acad. Sci. U. S. A. 107 (19) (2010) 8689–8694.
[49] H. Stroud, M.V. Greenberg, S. Feng, Y.V. Bernatavichute, S.E. Jacobsen, Comprehensive analysis of silencing mutants reveals complex regulation of the Arabidopsis methylome, Cell 152 (1–2) (2013) 352–364.
[50] T. Keller, J. Abbott, T. Moritz, P. Doerner, Arabidopsis regulator of axillary meristems1 controls a leaf axil stem cell niche and modulates vegetative development, Plant Cell 18 (3) (2006) 598–611.
[51] Y. Guo, S. Gan, AtMYB2 regulates whole plant senescence by inhibiting cytokinin-mediated branching at late stages of development in Arabidopsis, Plant Physiol. 156 (3) (2011) 1612–1619.
[52] J.T. Bell, A.A. Pai, J.K. Pickrell, D.J. Gaffney, R. Pique-Regi, J.F. Degner, Y. Gilad, J.K. Pritchard, DNA methylation patterns associate with genetic and gene expression variation in HapMap cell lines, Genome Biol. 12 (1) (2011) R10.
[53] Z. Lang, Y. Wang, K. Tang, D. Tang, T. Datsenka, J. Cheng, Y. Zhang, A.K. Handa, J. K. Zhu, Critical roles of DNA demethylation in the activation of ripening-induced genes and inhibition of ripening-repressed genes in tomato fruit, Proc. Natl. Acad. Sci. U. S. A. 114 (22) (2017) E4511–E4519.
[54] H. Wang, G. Beyene, J. Zhai, S. Feng, N. Fahlgren, N.J. Taylor, R. Bart, J. C. Carrington, S.E. Jacobsen, I. Ausin, CG gene body DNA methylation changes and evolution of duplicated genes in cassava, Proc. Natl. Acad. Sci. 112 (44) (2015) 13729–13734.
[55] Q.X. Song, X. Lu, Q.T. Li, H. Chen, X.Y. Hu, B. Ma, W.K. Zhang, S.Y. Chen, J. S. Zhang, Genome-wide analysis of DNA methylation in soybean, Mol. Plant 6 (6) (2013) 1961–1974.
[56] Y. Zhang, C. Liu, H. Cheng, S. Tian, Y. Liu, S. Wang, H. Zhang, M. Saqib, H. Wei, Z. Wei, DNA methylation and its effects on gene expression during primary to secondary growth in poplar stems, BMC Genomics 21 (1) (2020) 498.